International Journal of Pharmaceutics xxx (xxxx) xxx

Contents lists available at ScienceDirect

International Journal of Pharmaceutics

journal homepage: www.elsevier.com/locate/ijpharm

3D screen printing – An innovative technology for large-scale manufacturing of pharmaceutical dosage forms

Daniel Moldenhauer [a], Doan Chau Yen Nguyen [a], Lisa Jescheck [a], Franz Hack [b], Dagmar Fischer [c], Achim Schneeberger [a,*]

[a] Laxxon Medical GmbH, Hans-Knöll-Str. 6, 07745 Jena, Germany
[b] Pharmaceutical Technology and Biopharmacy, Institute of Pharmacy, Friedrich Schiller University Jena, Lessingstr. 8, 07743 Jena, Germany
[c] Pharmaceutical Technology, Department of Chemistry and Pharmacy, Friedrich-Alexander-Universität Erlangen-Nürnberg (FAU), Cauerstr. 4, 91058 Erlangen, Germany

ARTICLE INFO

Keywords:
3D printing
Additive manufacturing
Controlled release
Paracetamol
3D screen printing
Drug delivery system

ABSTRACT

Three-dimensional (3D) screen printing was used to fabricate oral dosage forms of different geometry and size. The paste required as starting material for the 3D screen printing process was designed for delayed release and contained the model drug paracetamol (acetaminophen). A prototype screen printing unit was used to fabricate different tablets in a single production process. The resulting tablets were produced with three different sizes and designed geometries (disk, donut, cuboid, oval and grid). Investigation of size and mass of the individual tablets demonstrated high uniformity within the various groups of tablets. Further characterization of their physical properties, such as breaking force and friability, yielded results comparing favorably to conventionally produced tablets. Finally, drug release tests in artificial gastric media showed paracetamol release to depend on the surface-area-to-volume ratio. In conclusion, the study shows the potential of 3D screen printing to fabricate more complex oral dosage forms in the setting of mass production with high reproducibility.

1. Introduction

3D printing (3DP) is an umbrella term that encompasses a range of different printing technologies (Chandekar et al., 2019; Gibson et al., 2015; Jacob et al., 2020). Prominent 3DP examples are binder jetting (also known as drop-on-powder) (Trenfield et al., 2018), fused deposition modelling (FDM) (Awad et al., 2018), semi-solid extrusion (also known as pressure-assisted microsyringe printing) (Firth et al., 2018), selective laser sintering (SLS) (Awad et al., 2020) and stereolithography (SLA) (Martinez et al., 2018). Their common and defining feature is the principle of additive manufacturing. However, they differ fundamentally in key aspects including the physical mechanisms used to deposit materials into layers and to cure them.

Additive manufacturing offers a series of advantages over conventionally used methods in the fabrication of drug delivery systems (DDS). These include the flexibility in the design of DDS with regard to geometry, size, content and release characteristics of the active pharmaceutical ingredient (API) (Chen et al., 2020). Moreover, layer-by-layer fabrication exploits all of the above advantages not only for DDS containing a single API but even in multi-drug formats. Noteworthy is also the fact that 3DP realizes all of these features within the very same production process. Finally, the required process conditions and generated DDS characteristics apply regardless of the batch size.

Never before has the pharmaceutical industry faced such a transformative manufacturing technology (Beg et al., 2020; Trenfield et al., 2019). Indeed, it could be utilized throughout the drug development process, offering high flexibility for DDS design during pre-clinical development and enabling different batch sizes of DDS with tailored doses/API release profiles covering small first-in-human clinical trials as well as larger studies and even front-line medical care. Perhaps even more important are the implications for the way we use medicines. 3DP could pave the way for personalized medicine through easy availability of DDS with tailored doses and API release profiles (Durga Prasad Reddy and Sharma, 2020). Potential scenarios range from a limited number of DDS variants covering clinically relevant patient groups to on-demand dispense for individual patients at the point of sale. Digitalization would support all of these approaches, which, at least in certain scenarios, would challenge the traditional way how drugs are developed,

* Corresponding author.
E-mail address: as@laxxon-medical.com (A. Schneeberger).

https://doi.org/10.1016/j.ijpharm.2020.120096
Received 25 September 2020; Received in revised form 11 November 2020; Accepted 12 November 2020
Available online 18 November 2020

approved and marketed (Khairuzzaman, 2018; Mirza and Iqbal, 2018). Most demanding, likewise for both the industry and regulators, would be the on-demand DDS fabrication for individual patients, representing a deep paradigm shift.

The use of 3DP technologies has been widely studied for the manufacture of DDS. All of the technologies listed above have been successfully used to produce DDS covering a broad range of APIs and drug release profiles including quick, delayed and extended release (Alhnan et al., 2016). However, to date there is only one 3D printed medicine, Spritam®, that is FDA approved and marketed (West and Bradbury, 2018). It is an antiepileptic based on a highly porous structure, achieved by a binder jetting technology termed ZipDose® (Yoo et al., 2014). Not surprisingly, it follows the conventional path of drug development, i.e. mass production and delivery of tablets for the entire population. Its key feature, rapid disintegration with fast API release, perfectly matches the intended use as an emergency medication and takes full advantage of the binder jetting technology. Given this situation, scalability and tangible patient benefits appear to be critical for a successful business case in the pharmaceutical industry. However, throughput is the primary limitation of most 3DP technologies, in particular extrusion- and laser-based approaches. Depending on the 3DP technology, other limitations include low mechanical resistance, low printing resolution and limited material choices (El Aita et al., 2018).

We report here the first study on 3D screen printing in the fabrication of DDS. 3D screen printing is not only offering all the advantages of additive manufacturing, but is set to overcome the limitations of the "conventional" 3DP technologies summarized above. In particular, we would position 3D screen printing as best suited for mass customization of DDS relying on a conventional regulatory strategy. In 3D screen printing, a screen mesh is used to transfer a semi-solid, API containing paste onto a substrate, except in areas made impermeable to the paste by a blocking stencil. The deposited layer is then dried. The next layer is printed precisely on top of the previous one after lifting the screen by the dried layer thickness. Regarding throughput, the number of units printed simultaneously is largely defined by the ratio of screen size to unit size. The cyclic process of 3D screen printing is based on the classic flatbed screen printing process (Bauer and Bauer, 1993), which finds wide applications in industry for textile prints, large-format posters, traffic routing systems and signs, electronic circuit boards, membrane switches, electronic display boards and solar cell electrodes (Kipphan, 2001; Lin, 2016). More recently, 3D screen printing has been used in the development of ceramic and metal parts for small series industrial applications. The studies presented by researchers of the Fraunhofer Institute for Manufacturing Technology (IFAM) demonstrated the power of the 3D screen printing technology for generating fine structures and parts with high resolution and precision even when using two different materials across different layers or within one and the same layer (Riecker et al., 2014; Jurisch et al., 2015; Studnitzky et al., 2016).

In the following work, we addressed basic aspects of the 3D screen printing technology in the context of DDS fabrication. To this end, DDS of different geometries and sizes were printed based on a paste designed to yield a delayed API release. Results of standard analytics of the printed products established the feasibility of the approach, thus providing proof-of-concept.

2. Materials and methods

2.1. Chemicals

Paracetamol (acetaminophen) was obtained from Alfa Aesar (Lancashire, UK). It was ground with a planetary ball mill and sieved through a 90 μm analytical sieve. Polyvinylpyrrolidone (PVP K30, 40,000 g/mol) was purchased from SERVA (Heidelberg, Germany) and glycerol (100%) from AppliChem (Darmstadt, Germany). Hydroxypropyl methylcellulose (HPMC, Benecel K4M Pharm CR, 340,000 g/mol) was kindly provided by Ashland (Covington, KY, USA) and starch 1500 by Colorcon (Dartford, UK). Sunflower oil was a commercially available food store grade. Milli-Q water (18.2 MΩ cm) was used for all formulations and solutions.

2.2. Preparation of printing paste

The paste was formulated according to the composition in Table 1 under room temperature conditions. HPMC with the necessary amount of water was processed to yield a 4 wt% gel solution. PVP was dissolved separately in water to which glycerol and sunflower oil were added subsequently under vigorous stirring with a magnetic stirrer. This mixture was then added to the 4 wt% HPMC gel under stirring with the overhead stirrer Hei-TORQUE Precision 400 (Heidolph Instruments GmbH & CO. KG, Schwabach, Germany) equipped with a spiral impeller. The next step involved the portion-wise addition of the paracetamol powder under constant stirring. In the last step, the starch powder was added in the same way and thorough stirring/mixing (30 min, 400 rpm) provided a homogeneous and smooth paste.

2.3. 3D screen printing of tablets

The lateral tablet dimensions are determined by the used screen layout (Fig. 2) and are given for each geometry and size in Table S1. Tablets were fabricated on a prototype inline production unit EX301i from Exentis Group AG as depicted in Fig. S1. Machine preparation for the printing process included mounting and alignment of the screen and the squeegees as well as the software set-up. Printer settings were as follows: flooding and printing squeegee speed 80 mm s^{-1}, off-contact distance 2 mm, height increment for screen elevation 20 μm, dryer temperature 85 °C and drying time per layer 28 s. Using these settings, 100 layers were printed. Tablets were printed on tempered glass plates (300 × 300 × 5 mm) with satin-finished surface. After printing was completed, the tablet-holding glass plates were further air-dried at room temperature overnight before the tablets could be easily removed with a razor blade. In this lab-scale run, we intended to print about 1000 tablets. To this end, the printer was equipped with 7 glass plates. Screens were designed to carry the 5 selected tablet geometries (disk, donut, cuboid, oval and grid) at 3 different sizes; a total of 10 units were represented per geometry and size. The area of the printing plate occupied by the tablets was about 40% of the overall printable plate area. Using this research and development set-up, the overall batch size was 1050 tablets (70 tablets of each geometry and size; 5 different geometries × 3 different sizes × 10 units per plate × 7 plates). The entire process (printing and drying) took 6.5 h.

2.4. Characterization of tablet morphology and mass uniformity

The weight of ten 3D screen-printed tablets (of each shape and size) was determined with an analytical fine balance. In addition, their geometry defining dimensions were individually measured with a digital caliper (diameter *D* for disk and donut, width *W* and length *L* for cuboid, oval and grid). The surface area *SA*, volume *V*, surface-area-to-volume-ratio *SA/V* and density ρ of the tablets were calculated based on these measured values. The average and standard deviation were calculated.

Table 1
Composition of the used printing paste.

Component	Wt%
Paracetamol	4.1
PVP K30	2.1
Starch 1500	14.4
Glycerol 100%	1.5
Sunflower oil	1.0
HPMC K4M	1.9
MilliQ Water	75.0
Total	*100.0*

2.5. Tablet hardness and friability testing

The hardness of three 3D screen-printed tablets (of each shape and size) was measured with the hardness tester TBH 30 (Erweka, Germany). For friability testing ten tablets (of each shape with size L) were brushed and accurately weighted (initial weight). Then, tablets were placed in the friability tester TAR 20 (Erweka, Germany) and rotated 100 times at a constant speed of 25 rpm. The tablets were brushed to remove any loose dust and reweighted (final weight), and the weight loss in % was calculated.

2.6. Dissolution testing

Dissolution profiles for the selected tablet geometry and size were obtained in triplicates on a Pharmatest PTWS 600 dissolution bath using a USP apparatus 2 setup. In each assay, the tablet was placed at the bottom of the vessel in 500 mL artificial gastric fluid (pH 1.2; prepared as follows: 1 g NaCl + 3.5 mL 37% HCl + 496.5 mL MilliQ water; this represents simulated gastric fluid in a composition according to USP XXII) under constant paddle stirring (50 rpm) at 37 °C. During the dissolution test, samples of 2 mL were manually drawn by pipette at defined time intervals and filled in centrifugation vials. The volume of removed sample media was replaced by the same amount of fresh dissolution media. Then, samples were centrifuged (10,000 rpm, 5 min) to remove insoluble tablet particles (Starch 1500) interfering with absorption measurements. The absorption of the supernatant was determined at $\lambda_{max} = 243$ nm with a Beckmann DU 640 spectrophotometer. The paracetamol concentration of samples was calculated from a previously recorded calibration curve (Fig. S2) also accounting for the dilution during the progressing test intervals. Tests were conducted in triplicates. Data are reported throughout as average ± standard deviation.

2.7. Determination of drug content and content uniformity

The paracetamol content in the printed tablets was determined from 3 tablets of each shape with size L at the end of dissolution testing. Therefore, the tablets were weighted with an analytical fine balance before starting dissolution testing and a sample from the dissolution bath after complete tablet disintegration and dissolution (usually after more than 24 h) was taken. Sample processing and measurement were as described in Section 2.6. The projected API content was calculated from the tablet mass and the 16.4 wt% of paracetamol, referring to the solid components of the printing paste. The average and standard deviation were calculated.

3. Results and discussion

3.1. Printing tablets of different geometry and size

3D screen printing is an additive manufacturing technology, i.e. objects are produced layer-by-layer. Accordingly, manufacturing involves the repetition of defined cycles. Each of these cycles can be divided into different steps. The cycle starts by positioning the printing screen in an off-contact distance above the substrate plate (Fig. 1a). Then, the API-containing paste is moved with the help of a flooding squeegee across the screen to fill the open mesh apertures (Fig. 1b). In a reverse printing stroke, the paste and tensioned screen mesh are brought into contact with the substrate along the line of the printing squeegees edge (Fig. 1c). Behind the squeegee, the screen snaps back to its initial position whereas the paste, through adhesion, remains on the substrate (Fig. 1d). Before printing the next layer on top, the substrate plate with the printed layer is transported to an external dryer to dry the printed layer, i.e. to remove paste solvents. Drying is achieved by convection with dry and heated air. Thereafter, the substrate plate returns to the printing station, where the printing screen is lifted by the thickness of the printed layer and the substrate plate is aligned beneath the screen to precisely match the now dried tablet layers with the open mesh apertures. Then, the cycle starts all over again and is repeated until the desired tablet height is reached.

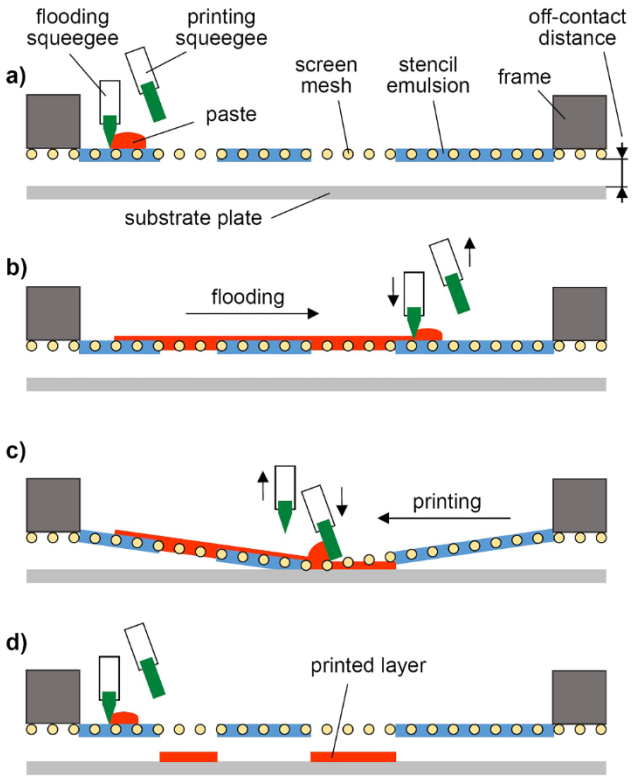

Fig. 1. Schematic representation of the different steps of the printing cycle. (a) Initial state with paste deposited on the screen, (b) distribution of paste across the screen to fill open areas (flooding), (c) printing on the substrate, (d) final state with printed layer simultaneously being the initial state for the subsequent layer.

3D screen printing is based on the transfer of the API-containing printing paste through distinct openings of the printing screen onto a given substrate. The layout of the printing screen can be designed in a flexible manner, for example to accommodate multiple units of a single geometry and size or, alternatively, multiple units of different geometries and sizes. Experiments reported here were done using a screen layout that allowed manufacturing of tablets of 5 different geometries (disk, donut, cuboid, oval and grid) each in 3 different sizes (small, medium, large) during the same production process (Fig. 2). The lateral tablet dimensions (diameter *D*, length *L*, width *W*) are defined by the size of the respective 2D layouts on the printing screen. In contrast, the tablet height *H* is a function of the number of printed layers and their thickness.

Using the paste designed to mediate delayed release of paracetamol (Table 1) and the printing screen shown in Fig. 2, we applied 100 printing cycles each delivering layers of 20 µm in thickness. Resulting tablets are shown in Fig. 3.

3.2. Physical properties of printed tablets

The designed lateral tablet dimensions in the current series of experiments were integral millimeter values for all tablet geometries (Table S1), e.g. disk L ($D = 8$ mm) or cuboid L ($L \times W = 10 \times 5$ mm). Measured sizes of the various printed tablet shapes are summarized in Table 2. With regard to lateral dimensions, the measured ones were somewhat smaller than those defined by the layout of the printing screen. On average, printed lateral sizes differed from the designed ones

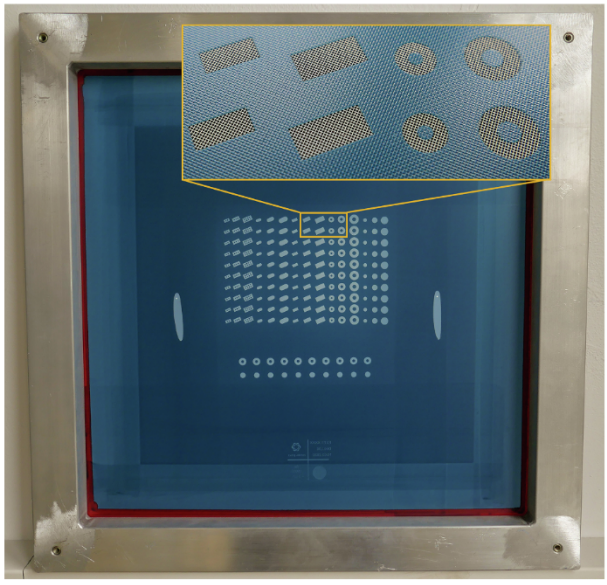

Fig. 2. Screen layout for various tablet geometries in different sizes. For the printing process, a screen with tensioned mesh is used to transfer printing paste onto a substrate, except in areas made impermeable to the paste by a blocking stencil made of a hardened photopolymeric emulsion. In this example, the mesh is white. Accordingly, white areas represent the tablet geometry to be printed. The hardened polymeric emulsion, rendering the mesh impermeable to the paste, is blue in this case. The magnifying inlet shows some tablet geometries and the mesh in more detail. The used screen measures 584 × 584 mm with a printing area of 180 × 180 mm and is designed to accommodate 10 tablets of 5 different geometries each in 3 sizes. (For interpretation of the references to colour in this figure legend, the reader is referred to the web version of this article.)

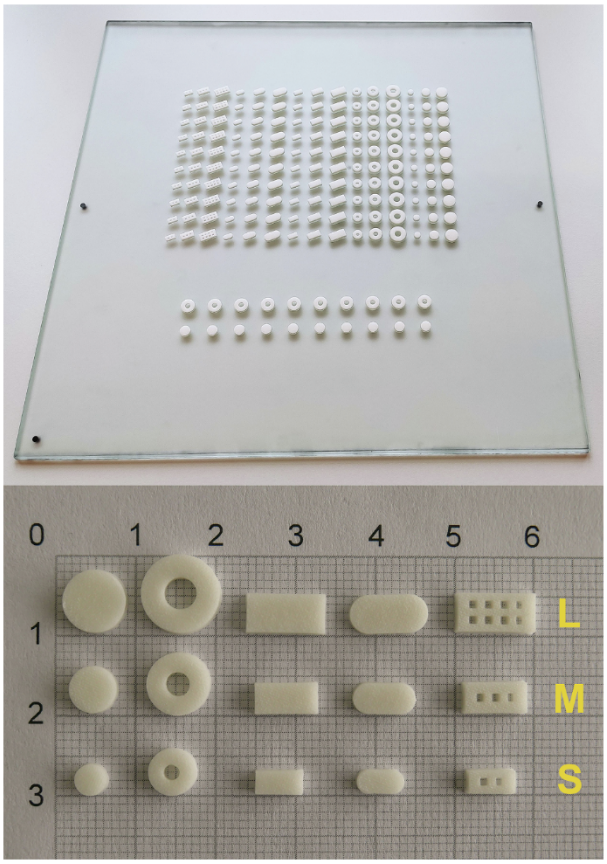

Fig. 3. Photographs of the 3D screen-printed tablets on the substrate plate (top) and on millimeter paper (bottom). The tablet shapes on millimeter paper are from left to right disk, donut, cuboid, oval and grid in a large (L), medium (M) and small (S) size (from top to bottom).

by up to −3%. As far as the height was concerned, deviation did not exceed −6%. Of note, the example provided shows a tendency for the height to decrease from the side of the disks to the side of the grids likely indicating a slight skewing of the printing screen. Nevertheless, the provided data demonstrate the high precision of 3D screen printing. The reduction in size results from water evaporation occurring during the drying process. Obviously, measures for size correction would differ for lateral dimensions and for height. Lateral dimensions are fixed by the layout of the printing screen. Corrections would require a new screen with unit size adapted for the expected shrinkage based on the water content of the printing paste. By contrast, height is controlled by the number and thickness of layers and can be regulated within the running printing process.

Measurement of tablet mass demonstrated standard deviations of no tablet group (defined by shape and size) to differ by more than 2.7% from the mean (oval S). As far as the percentage deviation of the individual tablets is concerned, this was in any case less than 6%. Of note, regarding deviation of individual tablets, larger tablets showed less deviation from the mean than the smaller tablets, 4.5% versus 6%, respectively. Data show that tablets with a high degree of mass uniformity can be produced using the 3D screen printing technology presented. In terms of reproducibility of geometry and size as well as mass uniformity, 3D screen printing delivers results with the same high level of quality as other 3D printing techniques (Goyanes et al., 2015a; Khaled et al., 2018; Martinez et al., 2018; Korte and Quodbach, 2018). Most importantly, results obtained comply with relevant regulatory requirements (Council of Europe, 2014). Specifically, the specifications given by the Eur. Ph. for uncoated tablets allow deviations of up to ±7.5% for average mass for tablets of 81–249 mg, and up to ±10% for average mass for tablets ≤ 80 mg (Council of Europe, 2014).

The hardness testing revealed (Table S2), that not all tablets, especially not those with a non-circular base area, could be broken into two parts by the testing equipment. Here, the moveable jaw of the apparatus rather bruised the tablet than crushed it. The donut tablets of all sizes have a constant breaking force of around 60 N. In contrast, the breaking force for the disks increases with size from about 100 N for size S to about 200 N for size L. Overall, the breaking force appears to be high and the printed tablets showed a high resistance to crushing. While in a conventional tablet press the breaking force can be influenced by the compression force, in 3D screen printing the tablet hardness mostly depends on the formulation composition and to some extent on the drying process. Given the robustness of the printed tablets, their percentage weight loss from friability testing was extremely low with less than 0.1% abrasion for the tested tablets (Table S3). In summary, it can be concluded that the physical tablet properties of 3D screen-printed tablets are by no means of less quality than that of conventionally pressed tablets.

3.3. Paracetamol content of printed tablets

Paracetamol content of printed tablets is primarily a function of the paracetamol content in the printing paste. Therefore, the paracetamol content was quantified after dissolution by spectrophotometric measurement. In the present case, the weight percentage of paracetamol in the paste was 4.1 wt%. Referring only to the solid components of the paste, the paracetamol content was 16.4 wt%. Printed tablets of all geometries and sizes were found to contain 99.5 ± 2.1% of the projected amount of paracetamol (Table 3). Thus, also with regard to API content, the presented 3D screen printing technology yields highly uniform results. Of note, in further experiments we were able to increase the paracetamol content of the paste to 33% (based on solid paste

Table 2
Physical parameters of printed tablets: Diameter D (outer, inner), length L, width W, height H, surface area SA, volume V, surface-area-to-volume-ratio SA/V, mass m and density ρ. Ten tablets of each geometry and size were weighted and measured with a digital caliper. V, SA/V and ρ were calculated applying the relevant formulae. All values are given as average with standard deviation.

Shape (Size)	D [mm]		H [mm]	SA [mm^2]	V [mm^3]	SA/V [mm^{-1}]	m [mg]	ρ [mg mm^{-3}]
Disk (L)	7.76 ± 0.03		2.06 ± 0.03	144.8 ± 1.4	97.4 ± 2.0	1.49 ± 0.02	98.5 ± 1.6	1.01 ± 0.03
Disk (M)	5.78 ± 0.03		2.03 ± 0.05	89.3 ± 1.1	53.2 ± 1.3	1.68 ± 0.02	55.3 ± 1.1	1.04 ± 0.02
Disk (S)	3.85 ± 0.04		2.10 ± 0.05	48.5 ± 0.9	24.3 ± 0.7	2.00 ± 0.02	25.2 ± 0.5	1.04 ± 0.02
Shape (Size)	D_o [mm]	D_i [mm]	H [mm]	SA [mm^2]	V [mm^3]	SA/V [mm^{-1}]	m [mg]	ρ [mg mm^{-3}]
Donut (L)	9.69 ± 0.05	3.89 ± 0.04	2.03 ± 0.04	210.1 ± 2.6	125.4 ± 3.1	1.68 ± 0.02	130.7 ± 1.2	1.04 ± 0.02
Donut (M)	7.74 ± 0.04	2.88 ± 0.06	2.03 ± 0.05	148.8 ± 1.7	82.3 ± 1.9	1.81 ± 0.02	84.6 ± 1.3	1.03 ± 0.02
Donut (S)	5.75 ± 0.04	1.96 ± 0.07	2.03 ± 0.05	95.1 ± 1.8	46.6 ± 1.7	2.04 ± 0.04	49.4 ± 0.4	1.06 ± 0.03
Shape (Size)	L [mm]	W [mm]	H [mm]	SA [mm^2]	V [mm^3]	SA/V [mm^{-1}]	m [mg]	ρ [mg mm^{-3}]
Cuboid (L)	9.76 ± 0.05	4.85 ± 0.04	2.03 ± 0.04	154.0 ± 1.9	96.0 ± 2.4	1.61 ± 0.02	97.1 ± 1.0	1.01 ± 0.03
Cuboid (M)	7.81 ± 0.01	3.88 ± 0.03	1.97 ± 0.07	106.6 ± 1.7	59.7 ± 2.1	1.79 ± 0.04	61.4 ± 1.2	1.03 ± 0.02
Cuboid (S)	5.84 ± 0.04	2.92 ± 0.03	1.95 ± 0.03	68.3 ± 0.6	33.3 ± 0.5	2.05 ± 0.01	33.9 ± 0.6	1.02 ± 0.02
Shape (Size)	L [mm]	W [mm]	H [mm]	SA [mm^2]	V [mm^3]	SA/V [mm^{-1}]	m [mg]	ρ [mg mm^{-3}]
Oval (L)	9.70 ± 0.02	4.83 ± 0.06	1.96 ± 0.04	132.8 ± 1.1	82.2 ± 1.6	1.61 ± 0.02	83.3 ± 1.4	1.01 ± 0.02
Oval (M)	7.77 ± 0.02	3.89 ± 0.05	1.89 ± 0.04	91.5 ± 0.9	50.7 ± 1.2	1.80 ± 0.03	52.1 ± 1.1	1.03 ± 0.02
Oval (S)	5.78 ± 0.02	2.96 ± 0.06	1.88 ± 0.07	57.8 ± 1.1	28.1 ± 1.1	2.06 ± 0.04	29.4 ± 0.8	1.05 ± 0.03
Shape (Size)	L [mm]	W [mm]	H [mm]	SA [mm^2]	V [mm^3]	SA/V [mm^{-1}]	m [mg]	ρ [mg mm^{-3}]
Grid[a] (L)	9.81 ± 0.04	4.99 ± 0.07	1.88 ± 0.04	197.0 ± 3.1	78.0 ± 2.2	2.53 ± 0.03	78.5 ± 1.2	1.01 ± 0.03
Grid[a] (M)	7.83 ± 0.01	3.94 ± 0.08	1.86 ± 0.03	121.5 ± 1.3	52.1 ± 1.0	2.33 ± 0.02	53.7 ± 0.6	1.03 ± 0.02
Grid[a] (S)	5.85 ± 0.02	2.94 ± 0.02	1.81 ± 0.02	76.6 ± 0.7	27.8 ± 0.5	2.76 ± 0.02	29.3 ± 0.5	1.05 ± 0.01

[a] Grid cavities have a squared base area of edge length 0.98 ± 0.02 mm. The number of grid cavities are 8 for size L, 3 for size M and 2 for size S.

Table 3
Paracetamol content of 3D printed tablets of various forms and sizes with 16.4 wt% paracetamol. Projected API content reflects to the amount of paracetamol as defined by the wt% of paracetamol, referring to the solid components of the printing paste, and the mass of a given tablet.

API content	Disk (L)	Donut (L)	Cuboid (L)	Oval (L)	Grid (L)
$m_{projected}$ [mg]	16.2 ± 0.3	21.7 ± 0.2	15.9 ± 0.1	13.4 ± 0.2	12.9 ± 0.2
$m_{measured}$ [mg]	16.0 ± 0.0	21.4 ± 0.1	15.7 ± 0.1	13.5 ± 0.5	12.7 ± 0.1
$m_{measured}/m_{projected}$ [%]	98.7 ± 1.6	98.4 ± 0.5	99.2 ± 0.3	100.6 ± 3.6	98.3 ± 1.2

components) and use it to print uniform tablets releasing the expected amount of drug (Table S4).

3.4. Dissolution studies

To further characterize the printed tablets, they were subjected to dissolution testing in acidic solution at pH 1.2 resembling artificial stomach conditions. In this regard, it is important to note, that all tablets, regardless of their geometry and size, had been manufactured using the same printing paste and under the same conditions. Thus, paracetamol release profiles of different tablet geometries/sizes should follow the general rules of drug release, namely, correlation of the rate of release with the surface-area-to-volume ratio (SA/V ratio). It is well established that the higher the SA/V ratio, the faster the release of the active pharmaceutical ingredient (Brooke and Washkuhn, 1977; Ford et al., 1987; Reynolds et al., 2002). To this end, we first compared tablets with comparable mass but different SA/V ratio and shape. Specifically, paracetamol release profiles of grid, oval and disk geometry, each in medium size, were investigated (Fig. 4). As expected, rate of drug release paralleled the SA/V ratios with fastest release seen with the grid geometry, which had the highest SA/V ratio in this series. Next, release profiles of tablets with similar SA/V ratios but different shape and mass were examined (Fig. 5). Here, it is evident for both examples, that the dissolution profiles overlap almost completely and are considered to be similar according to a similarity factor (f_2) test (data see Table S5). Therefore, drug release from the 3D screen-printed tablets follows the general rules that govern drug release from solid oral dosage forms. Future studies will have to address the stability and physical state of the

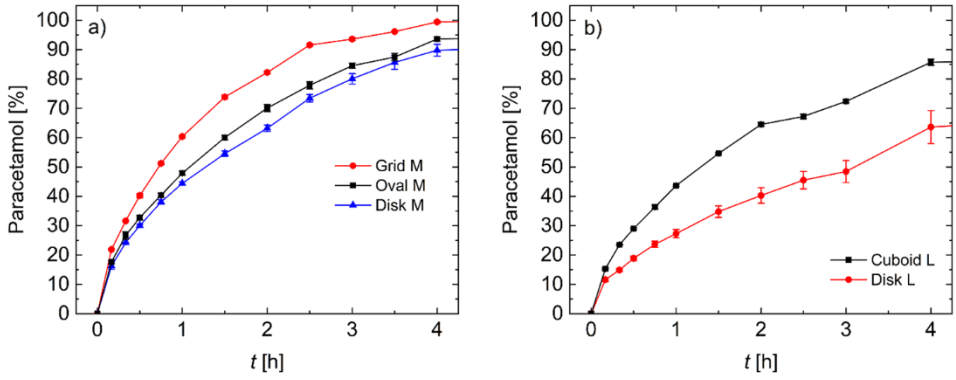

Fig. 4. Dissolution profiles of 3D screen-printed tablets with constant mass and different surface-area-to-volume-ratio. (a) $m \approx 54$ mg, $SA/V = 2.33$ (Grid M), 1.80 (Oval M), 1.68 (Disk M). (b) $m \approx 98$ mg, $SA/V = 1.61$ (Cuboid L), 1.49 (Disk L).

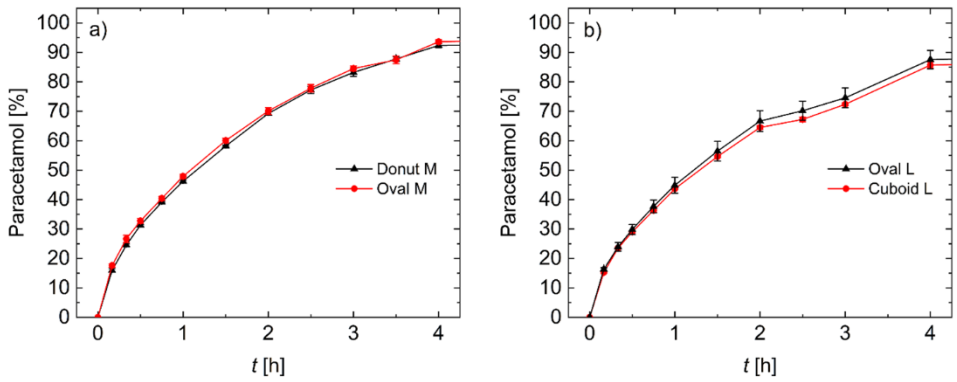

Fig. 5. Dissolution profiles of 3D screen-printed tablets with constant surface-area-to-volume-ratio and different mass. a) $SA/V \approx 1.80$, $m = 84.6$ mg (Donut M), 52.1 mg (Oval M). b) $SA/V \approx 1.61$, $m = 83.3$ mg (Oval L), 97.1 mg (Cuboid L).

drugs as well as the behavior of the screen-printed DDS in different release media with varying pH. Regarding drug release profiles, 3D screen printing parallels the performance of other 3DP technologies including binder jetting, fused deposition modelling and semi-solid extrusion (Goyanes et al., 2015a, 2015b; Khaled et al., 2015, 2018). Thus, additive manufacturing technologies, including 3D screen printing, offer the unique advantage of conventional powder compaction of easy and stepwise modification of the geometry and size of oral dosage forms and thereby allow for the control of drug release.

Overall, the above findings provide proof-of-concept of the 3D screen printing technology for manufacturing of solid oral dosage forms.

3.5. Potential and outlook

Experiments summarized here are meant to provide a first and concise overview of basic aspects of the 3D screen printing technology. Obviously, further aspects are subject to ongoing studies. One of these topics is the fabrication of more complex DDS, a key domain of additive manufacturing technologies (Goyanes et al., 2015b; Fina et al., 2018). The possibility of producing DDS that harbor more than one API (Khaled et al., 2015), another strength of 3DP, is shown in Fig. S3. For demonstration purposes, we printed tablets with differently colored pastes. Their fabrication requires a switch between 2 printing pastes, which is most efficiently accomplished using two printing stations. Other ongoing studies address the choice of materials with regard to both, APIs and excipients. Initial studies indicate that the presented paste can accommodate other APIs including, but not limited to, dapsone (sulfone; antimicrobial and anti-inflammatory activity) and levodopa (dopamine precursor; Parkinson's disease). Similarly, other polymeric excipients such as microcrystalline cellulose, crospovidone, carboxymethyl cellulose or hydroxyethyl cellulose have been successfully used for paste formulation and in printing (data not shown). Pastes generated with these polymers differ from the presented one by the rate of drug release. For example, microcrystalline cellulose, crospovidone and a low molecular weight binder polymer form the base for a paste yielding immediate release dosage forms. Critical paste attributes are viscoelastic properties and the particle size of insoluble paste components. Concerning the former, the resting viscosity of the paste should be in a range, so that the wet printed layers do not spread through gravity, and the paste should possess adequate shear thinning behavior for the squeegee process. For insoluble paste components, the particle size is determined by the mesh openings and should be smaller by a factor of approximately 3.

We anticipate the choice of materials in the setting of 3D screen printing to compare favorably to "conventional" 3DP technologies as manufacturing conditions are relatively mild (Alhnan et al., 2016; Palo et al, 2017). With regard to scalability, 3D screen printing differs substantially from the "conventional" 3DP technologies, which are limited by the number of printing heads building up one tablet unit at a time (Alhnan et al., 2016; Hsiao et al., 2018). It allows simultaneous build-up of thousands of units through one screen. The capacity of a given screen is defined by its size and the size of the DDS. As a rule of thumb, the output is roughly defined by the ratio of screen size to DDS size with some influence of the form of the DDS: maximal DDS numbers are achieved with rectangular shapes, while the disk form is at the lower end in this regard. We currently use a screen size of 584 × 584 mm, which can be scaled up to 1200 × 1200 mm. In terms of unit numbers, plates of this dimension can, depending on the size of the tablets to be printed, accommodate between 12,000 tablets, with a diameter of 10 mm, and 40,000 tablets with a diameter of 5 mm. The time to print a single layer is in the order of a few (3–5) seconds. Also, drying can be accomplished within seconds depending on the paste, layer thickness and drying temperature. Printing systems such as the EX 434i are equipped with 4 printing stations and can circulate up to 160 plates (according to the manufacturer). While these numbers give an idea, output is a function of various parameters, in particular the complexity of the DDS, and serious predictions require a case-by-case evaluation.

4. Conclusions

This is the first report on the use of 3D screen printing in the fabrication of drug delivery systems. The presented study is based on the model drug paracetamol being incorporated in a paste designed for delayed drug release. With this paste and a prototype 3D screen printing machine tablets of 5 different geometries and 3 different sizes were produced. With regards to typical pharmaceutical tablet properties such as mass uniformity, content uniformity, breaking force and friability, the oral dosage forms showed high comparability to conventional tableting and other 3D printing technologies. Dissolution testing confirmed a delayed paracetamol drug release, whose drug release rate was governed by the surface-area-to-volume ratio and thus the tablet geometry and size. Overall, the obtained results provide a proof-of-technology. Future studies will have to confirm and extend these initial results in various directions. These include the definition of the spectrum of drugs that can be accommodated in pastes, like the one presented, and the identification of pastes with different release profiles, e.g., immediate drug release. Other topics to be addressed are the stability and the physical state of the drugs within the 3D screen-printed DDS. The flexibility of the technology, with regards to the ease to manufacture tablets of different geometry and size, and the presented findings strongly support the use of 3D screen printing for manufacturing of innovative and more complex drug release systems in the setting of large-scale production.

CRediT authorship contribution statement

Daniel Moldenhauer: Conceptualization, Methodology, Validation, Investigation, Formal analysis, Data curation, Visualization, Writing - original draft. **Doan Chau Yen Nguyen:** Investigation, Validation, Data curation, Visualization. **Lisa Jescheck:** Investigation, Validation. **Franz Hack:** Resources. **Dagmar Fischer:** Supervision, Writing - review & editing. **Achim Schneeberger:** Conceptualization, Supervision, Project administration, Writing - review & editing.

Declaration of Competing Interest

The authors declare that they have no known competing financial interests or personal relationships that could have appeared to influence the work reported in this paper.

Acknowledgement

Financial support of the Thüringer Aufbaubank (TAB) is gratefully acknowledged.

Appendix A. Supplementary material

Supplementary data to this article can be found online at https://doi.org/10.1016/j.ijpharm.2020.120096.

References

Alhnan, M.A., Okwuosa, T.C., Sadia, M., Wan, K.W., Ahmed, W., Arafat, B., 2016. Emergence of 3D printed dosage forms: opportunities and challenges. Pharm. Res. 33, 1817–1832. https://doi.org/10.1007/s11095-016-1933-1.

Awad, A., Fina, F., Goyanes, A., Gaisford, S., Basit, A.W., 2020. 3D printing: Principles and pharmaceutical applications of selective laser sintering. Int. J. Pharm. 586, 119594 https://doi.org/10.1016/j.ijpharm.2020.119594.

Awad, A., Gaisford, S., Basit, A.W., 2018. Fused deposition modelling: Advances in engineering and medicine. In: Basit, A., Gaisford, S. (Eds.), 3D Printing of Pharmaceuticals. AAPS Advances in the Pharmaceutical Sciences Series, vol. 31. Springer, Cham, pp. 107–132. https://doi.org/10.1007/978-3-319-90755-0_6.

Bauer, J., Bauer, A., 1993. Process for producing moulded bodies with a predetermined pore structure. DE Patent 4205969.

Beg, S., Almalki, W.H., Malik, A., Farhan, M., Aatif, M., Rahman, Z., Alruwaili, N.K., Alrobaian, M., Tarique, M., Rahman, M., 2020. 3D printing for drug delivery and biomedical applications. Drug Discov. Today 25, 1668–1681. https://doi.org/10.1016/j.drudis.2020.07.007.

Brooke, D., Washkuhn, R., 1977. Zero-order drug delivery system: theory and preliminary testing. J. Pharm. Sci. 66, 159–162. https://doi.org/10.1002/jps.2600660206.

Chandekar, A., Mishra, D.K., Sharma, S., Saraogi, G.K., Gupta, U., Gupta, G., 2019. 3D printing technology: a new milestone in the development of pharmaceuticals. Curr. Pharm. Des. 25, 937–945. https://doi.org/10.2174/1381612825666190507115504.

Chen, G., Xu, Y., Kwok, P.C.L., Kang, L., 2020. Pharmaceutical applications of 3D printing. Addit. Manuf. 34, 101209 https://doi.org/10.1016/j.addma.2020.101209.

Council of Europe, 2014. European Pharmacopoeia, 8th ed. Council of Europe, Strasbourg.

Durga Prasad Reddy, R., Sharma, V., 2020. Additive manufacturing in drug delivery applications: a review. Int. J. Pharm. 589, 119820. https://doi.org/10.1016/j.ijpharm.2020.119820.

El Aita, I., Ponsar, H., Quodbach, J., 2018. A critical review on 3D-printed dosage forms. Curr. Pharm. Des. 24, 4957–4978. https://doi.org/10.2174/1381612825666181206124206.

Fina, F., Goyanes, A., Madla, C.M., Awad, A., Trenfield, S.J., Kuek, J.M., Patel, P., Gaisford, S., Basit, A.W., 2018. 3D printing of drug-loaded gyroid lattices using selective laser sintering. Int. J. Pharm. 547, 44–52. https://doi.org/10.1016/j.ijpharm.2018.05.044.

Firth, J., Basit, A.W., Gaisford, S., 2018. The role of semi-solid extrusion printing in clinical practice. In: Basit, A., Gaisford, S. (Eds.), 3D Printing of Pharmaceuticals. AAPS Advances in the Pharmaceutical Sciences Series, vol. 31. Springer, Cham, pp. 133–151. https://doi.org/10.1007/978-3-319-90755-0_7.

Ford, J.L., Rubinstein, M.H., McCaul, F., Hogan, J.E., Edgar, P.J., 1987. Importance of drug type, tablet shape and added diluents on drug release kinetics from hydroxypropylmethylcellulose matrix tablets. Int. J. Pharm. 40, 223–234. https://doi.org/10.1016/0378-5173(87)90172-4.

Gibson, I., Rosen, D., Stucker, B., 2015. Additive Manufacturing Technologies. Springer, New York. https://doi.org/10.1007/978-1-4939-2113-3.

Goyanes, A., Martinez, P.R., Buanz, A., Basit, A.W., Gaisford, S., 2015a. Effect of geometry on drug release from 3D printed tablets. Int. J. Pharm. 494, 657–663. https://doi.org/10.1016/j.ijpharm.2015.04.069.

Goyanes, A., Wang, J., Buanz, A., Martinez-Pacheco, R., Telford, R., Gaisford, S., Basit, A. W., 2015b. 3D printing of medicines: engineering novel oral devices with unique design and drug release characteristics. Mol. Pharm. 12, 4077–4084. https://doi.org/10.1021/acs.molpharmaceut.5b00510.

Hsiao, W.K., Lorber, B., Reitsamer, H., Khinast, J., 2018. 3D printing of oral drugs: a new reality or hype? Expert Opin. Drug Deliv. 15, 1–4. https://doi.org/10.1080/17425247.2017.1371698.

Jacob, S., Nair, A.B., Patel, V., Shah, J., 2020. 3D printing technologies: recent development and emerging applications in various drug delivery systems. AAPS PharmSciTech 21, 220. https://doi.org/10.1208/s12249-020-01771-4.

Jurisch, M., Studnitzky, T., Andersen, O., Kieback, B., 2015. 3D screen printing for the fabrication of small intricate Ti-6Al-4V parts. Powder Metall. 58, 339–343. https://doi.org/10.1179/0032589915z.000000000255.

Khairuzzaman, A., 2018. Regulatory perspectives on 3D printing in pharmaceuticals. In: Basit, A., Gaisford, S. (Eds.), 3D Printing of Pharmaceuticals. AAPS Advances in the Pharmaceutical Sciences Series, vol. 31. Springer, Cham, pp. 215–236. https://doi.org/10.1007/978-3-319-90755-0_11.

Khaled, S.A., Alexander, M.R., Irvine, D.J., Wildman, R.D., Wallace, M.J., Sharpe, S., Yoo, J., Roberts, C.J., 2018. Extrusion 3D printing of paracetamol tablets from a single formulation with tunable release profiles through control of tablet geometry. AAPS PharmSciTech 19, 3403–3413. https://doi.org/10.1208/s12249-018-1107-z.

Khaled, S.A., Burley, J.C., Alexander, M.R., Yang, J., Roberts, C.J., 2015. 3D printing of tablets containing multiple drugs with defined release profiles. Int. J. Pharm. 494, 643–650. https://doi.org/10.1016/j.ijpharm.2015.07.067.

Kipphan, H., 2001. Handbook of Print Media. Springer, Berlin, Heidelberg. https://doi.org/10.1007/978-3-540-29900-4.

Korte, C., Quodbach, J., 2018. 3D-printed network structures as controlled-release drug delivery systems: dose adjustment, API release analysis and prediction. AAPS PharmSciTech 19, 3333–3342. https://doi.org/10.1208/s12249-018-1017-0.

Lin, J., 2016. Printing processes and equipments. In: Cui, Z. (Eds.), Printed Electronics: Materials, Technologies and Applications. publisherJohn Wiley & Sons Singapore Pte. Ltd, pp. 116–118. https://doi.org/10.1002/9781118920954.ch4.

Martinez, P.R., Basit, A.W., Gaisford, S., 2018. The history, developments and opportunities of stereolithography. In: Basit, A., Gaisford, S. (Eds.), 3D Printing of Pharmaceuticals. AAPS Advances in the Pharmaceutical Sciences Series, vol. 31. Springer, Cham, pp. 55–79. https://doi.org/10.1007/978-3-319-90755-0_4.

Mirza, M.A., Iqbal, Z., 2018. 3D printing in pharmaceuticals: Regulatory perspective. Curr. Pharm. Des. 24, 5081–5083. https://doi.org/10.2174/1381612825666181130163027.

Palo, M., Holländer, J., Suominen, J., Yliruusi, J., Sandler, N., 2017. 3D printed drug delivery devices: perspectives and technical challenges. Expert Rev. Med. Devices 14, 685–696. https://doi.org/10.1080/17434440.2017.1363647.

Reynolds, T.D., Mitchell, S.A., Balwinski, K.M., 2002. Investigation of the effect of tablet surface area/on drug release from hydroxypropylmethylcellulose controlled-release matrix tablets. Drug Dev. Ind. Pharm. 28, 457–466. https://doi.org/10.1081/ddc-120003007.

Riecker, S., Studnitzky, T., Andersen, O., Kieback, B., 2014. 3D multi-material metal printing of delicate structures. Conference EURO PM2014, Salzburg. https://www.researchgate.net/publication/325421798_3D_Multi-Material_Metal_Printing_of_Delicate_Structures (accessed 23 September 2020).

Studnitzky, T., Dressler, M., Andersen, O., Kieback, B., 2016. 3D screen printing-mass production for metals, ceramics and its combinations. Fraunhofer Direct Digital Manufacturing Conference DDMC 2016, Berlin. https://www.researchgate.net/publication/328163934_3D_Screen_Printing-Mass_Production_for_Metals_Ceramics_and_its_Combinations (accessed 23 September 2020).

Trenfield, S.J., Madla, C.M., Basit, A.W., Gaisford, S., 2018. Binder jet printing in pharmaceutical manufacturing. In: Basit, A., Gaisford, S. (Eds.), 3D Printing of Pharmaceuticals. AAPS Advances in the Pharmaceutical Sciences Series, vol. 31. Springer, Cham, pp. 41–54. https://doi.org/10.1007/978-3-319-90755-0_3.

Trenfield, S.J., Awad, A., Madla, C.M., Hatton, G.B., Firth, J., Goyanes, A., Gaisford, S., Basit, A.W., 2019. Shaping the future: recent advances of 3D printing in drug delivery and healthcare. Expert Opin. Drug Deliv. 16, 1081–1094. https://doi.org/10.1080/17425247.2019.1660318.

West, T.G., Bradbury, T.J., 2018. 3D printing: A case of ZipDose® technology - world's first 3D printing platform to obtain FDA approval for a pharmaceutical product. In: Maniruzzaman, M. (Eds.), 3D and 4D Printing in Biomedical Applications. Wiley-VCH Verlag GmbH & Co. KGaA, pp. 53–79. https://doi.org/10.1002/9783527813704.ch3.

Yoo, J., Bradbury, T.J., Bebb, T.J., Iskra, J., Surprenant, H.L., West, T.G., 2014. Three-dimensional printing system and equipment assembly. US Patent 20140065194.